



Research article

Preparation and characterization of acetate cellulose electrospun nanofibers membrane: Potential application on wastewater treatment



Ines Elaissaoui^a, Soumaya Sayeb^a, Ibtissem Ounif^b, Mounir Ferhi^a,
Horchani-naifer Karima^a, Dorra Jellouli Ennigrou^{a,*}

^a Physical Chemistry Laboratory of Mineral Materials and Their Applications, National Center for Research in Materials Sciences, Technopark Borj Cedria, P.O. Box: 73-8027, Soliman, Tunisia

^b Laboratory of Water, Membrane and Environmental Biotechnology, Centre of Research and Water Technologies, Technopark of Borj-Cedria, BP 273, 8020, Soliman, Tunisia

ARTICLE INFO

Keywords:

Electrospinning
Nanofibers
Hydrophobicity
Indigo carmine
Nanofiltration

ABSTRACT

Development of nanofiber membranes with the ability to remove organic dye such as Indigo Carmine (IC) from effluent wastewater is of immense help to the textile industry. In the present study, we investigate the preparation of cellulose acetate (CA) nanofiber membranes with optimized performances using electrospinning technique for effective removal of Indigo Carmine (IC) dye. Electrospinning parameters and solvent system containing acetic acid were adjusted to obtain CA nanofibers membranes which better suits dye removal application. The obtained nanofiber membranes were characterized using Scanning Electron Microscopy (SEM), Fourier-Transform Infrared Spectroscopy (FT-IR) and contact angle analysis. Results show that nanofiber webs with optimized electrospinning parameters were continuously formed and are substantially free of defects such as beading, with an average diameter of 950 ± 50 nm. Hydrophobicity of membranes were successfully modified and showed important increase of contact angle values from 37° to 107° . The stirring time was varied to improve the solution homogeneity and consequently the response of membranes in filtration treatment. The CA membranes performance was evaluated through water flux and permeability measurement and tested on IC dye removal. The results showed a rate of dye removal around 83 % and a maximum adsorption capacity (Q_m) of 13.09 mg/g for the optimized CA membranes.

1. Introduction

Water pollution causes a severe issue concern to the environment and public health. Particularly, dye contamination caused several environmental issues that necessitate more attention [1]. Before being released into the environment, the effluent from printing and dyeing units must first undergo thorough treatment because it frequently contains residual of reactive colors and chemicals. Synthetic dyes include complex aromatic molecule structures which are considered extremely important to treat, before it is discharged into the environment [2,3]. Among many industrial dyes, indigo carmine (IC) is widely produced and used as a coloring dye in denim

* Corresponding author.

E-mail address: dorra.jellouli.1978@gmail.com (D.J. Ennigrou).

<https://doi.org/10.1016/j.heliyon.2024.e32552>

Received 21 September 2023; Received in revised form 24 May 2024; Accepted 5 June 2024

Available online 8 June 2024

2405-8440/© 2024 Published by Elsevier Ltd.

This is an open access article under the CC BY-NC-ND license

(<http://creativecommons.org/licenses/by-nc-nd/4.0/>).

production (a denim clothes requires 3–12 g of IC per pair). Nevertheless, it is considered toxic for environment and human. For this reason, textile wastewater effluents must be treated [4–6]. Traditional methods such as, precipitation, flocculation, coagulation, and biological processes have many limitations, making their dye removal less effective. Furthermore, these techniques have high energy requirements [7]. Recently, several treatment methods have been used to remove dyes from wastewaters via photocatalysis [8], advanced oxidation processes [9], adsorption [10], biological treatment [11], liquid membrane separation [12] and membrane filtration [13,14].

Among the used approaches, membrane filtration is regarded as one of the most advantageous in dye degradation processes. One of the most energy-efficient membrane filtration techniques is reverse osmosis (RO), which uses pressure to drive microfiltration (MF), ultrafiltration (UF), nanofiltration (NF). In contrast to distillation, which requires more energy, membrane filtration technique is relatively fast, efficient, cost effective and treats a wide range of organic pollutants [15]. For effective membrane filtration processes, the used membrane type is considered as a key element [16–18]. Polymeric membranes produced by the phase inversion method are relatively inexpensive, but they have an asymmetric structure which leads to low surface porosity as well as low permeability [19]. Materials with nanoscale dimensions received enormous attention due to their suitability for water-waste application [13]. The distinctiveness of nanomaterials relies not only on their large specific surface area, lightweight, adjustable morphology, and height porosity, but also on their good computability and easy modification with other functional materials [20–22]. Among several methods for nanomaterials fabrication, electrospinning demonstrated an effective method to prepare nanofiber materials [23,24]. In fact, electrospinning technique has created entirely new opportunities to nanomaterials, due to its effectiveness and simplicity. Electrospun membranes, due to their excellent advantages, were developed to successfully accomplish the filtration issues associated with ultrafine particles. These benefits include a small fiber diameter, a morphology that can be steered, a porous structure that can be controlled, a high specific surface area, and a good internal connectivity [25,26]. Electrospun fiber membranes, particularly in the field of wastewater treatment, have reduced the disadvantages of low efficiency, high energy use and challenges with recycling of traditional processes [27,28].

Numerous factors influence the electrospinning process and the form of the resulting fibers. The impacts of solution and process characteristics, including material composition, applied voltage, polymer concentration and tip-to-collector distance, on the resultant nanofibers were examined by several authors [29–31]. Among these parameters, the viscosity of the polymer solution has the greatest effect on the process and resulting fiber morphology [32]. Viscosity is dependent to the polymer concentration in electrospinning solution, the average molecular weight on the polymer and the solution surface tension [33]. The key parameter of the electrospinning technique for major applications is the diameter of the obtained nanofibers. It determines the structural characteristics, including pore size and pore size distribution. Subsequently, these characteristics have great impact on the filter's permeability and selectivity [34]. Up to date, much effort has been performed and according to the literature, electrospun CA membranes have been widely used in wastewater treatment fields. In fact, Zhang and Wong [2022] prepared a cellulose acetate/chitosan nanofibers membrane for Humic-Acid removal [27]. Mansourizadeh et al. [2014] fabricated cellulose acetate (CA), polyethersulfone (PES), and polyethylene glycol (PEG) membranes using phase-inversion process for oil removal. They attained a membrane rejection efficiency of 88 % for PES/CA membranes [35]. In the same regard, El-Barbary et al. [2021] developed a composite containing cadmium selenide (CdSe) modified with Ag ions and graphene oxide (GO) nanosheets and CA nanofibers to degrade the methylene blue (MB) dye using photocatalysis [33]. Concerning IC dye removal, Yazdi et al. [2018], prepared an amidoximated polyacrylonitrile (APAN) nanofibers surface coated with magnetite nanoparticles (Fe_3O_4 NPs) for this purpose [36]. In another research [37], modified PEG with hydroxyapatite nanoparticles was employed as a new and effective adsorbent for IC dye removal.

In the present study, the main objective is to synthesize electrospun neat CA membranes with optimized characteristics for IC dye removal. Indeed, CA polymer is selected to create nanowebs because of its superior mechanical capabilities, mass transfer, chemical stability, and capacity to produce nanofibers. During experimental, electrospinning parameters were varied, and acetic acid (AC) was selected as solvent and cross-linking agent for CA polymer to reduce its hydrophilic character. Moreover, stirring time was varied from 2 to 48 h at 25 °C to optimize the solution homogeneity.

The elaborated nanofibers were characterized by Scanning Electron Microscopy (SEM), Fourier-transform infrared (FT-IR) spectroscopy and contact angle measurements. After membrane synthesis and obtaining CA uniform nanofibers, membrane performance was evaluated by conducting water flux and permeability measurements. During research, the response of different CA prepared membranes to IC dye treatment were also evaluated using nanofiltration process. The color removal is designated as a treatment performance indicator for our assessment.

2. Materials and methods

2.1. Material

Cellulose Acetate polymer (acetyl content: 39.8 % (w/w), Mw 30,000 Da) was purchased from Sigma Aldrich. Acetic acid (from chamlab) was used as solvent. A Millipore Milli-Q water purification system with a resistivity of 18.2 M cm^{-1} , was used to produce ultra-pure water. Indigo carmine dye with a molecular formula $\text{C}_{16}\text{H}_8\text{N}_2\text{Na}_2\text{O}_8\text{S}_2$, acquired from Sigma Aldrich, was considered as dye pollutant. All chemical reagents and solvents in this work were used without further purification.

2.2. Preparation of cellulose membranes

During preliminary tests, an amount of 16 % CA concentration was fixed to obtain continuous nanofibers. Then, it was dissolved in

acetic acid, the mixture was stirred for varied time: 2 h, 24 h and 48 h at 25 °C until the electrospinning solution becomes homogenous. Under stirring, the solution was covered. Finally, the electrospinning solution was loaded into a 10 mL plastic syringe using a gauge needle. During electrospinning, a voltage of 18 kV was applied between the needle and the plate collector. To achieve the desirable highly porous shape, a flow rate of 2 mL per hour was maintained. The plate collector, covered with aluminum foil, was placed at 15 cm from the tip of the needle. The produced CA electrospun membrane was, first, dried under vacuum for 2 h at 60 °C to eliminate any remaining solvent, and then immersed in water for 2 h to effectively obtain individualized membrane. The preparation steps involved in this study are summarized in Fig. 1.

2.3. Membrane characterization

2.3.1. Fourier-transform infrared spectroscopy (FTIR)

Fourier-transform infrared spectroscopy (FTIR PerkinElmer spectrometer, serial number: 110,400) was used to determine the chemical structure of the produced membranes. FTIR spectra of CA membranes were measured in the wavenumbers range of 500–4000 cm^{-1} .

2.3.2. Contact angle measurements

The static water contact angle (WCA) of the elaborated membranes was measured using the contact angle meter (ATTENTION, THETA, serial number: S/N AAV 100005) to investigate the surface wettability of the electrospun membranes. For each sample, five readings of the water contact angle (WCA) were given at various points from the surface sample, and the average of these values was reported.

2.3.3. Morphological analysis

Using scanning electron microscopy (FEI Quanta 650 SEM, serial number: 9950170), the obtained nanofibrous morphology of membranes is examined.

2.4. Membrane performance

2.4.1. Water flux and permeability measurements

A stainless-steel cell (Millipore) was used to test the water flux and permeability, and N_2 gas was used to maintain the pressure. The effective membrane area was 38.54 cm^2 , and the filtration cell had a 350 mL capacity. The pure water flux was determined as a function of pressure (from 0 to 12 bar). The following equation was used to determine the permeate flux, which was measured as the volume of water permeating per unit area of membrane at specific time [38,39].

$$J_v = \frac{v}{At} \quad (1)$$

where J_v is the permeate flux ($\text{L m}^{-2} \text{h}^{-1}$), v the volume of permeate (L), A the membrane area (m^2) and t is the operating time (h).

The following equation uses Darcy's law to express the ultrapure water flux through the membrane (J_w):

$$J_w = L_p^0 \times \Delta P = \frac{\Delta P}{\eta \times R_m} \quad (2)$$

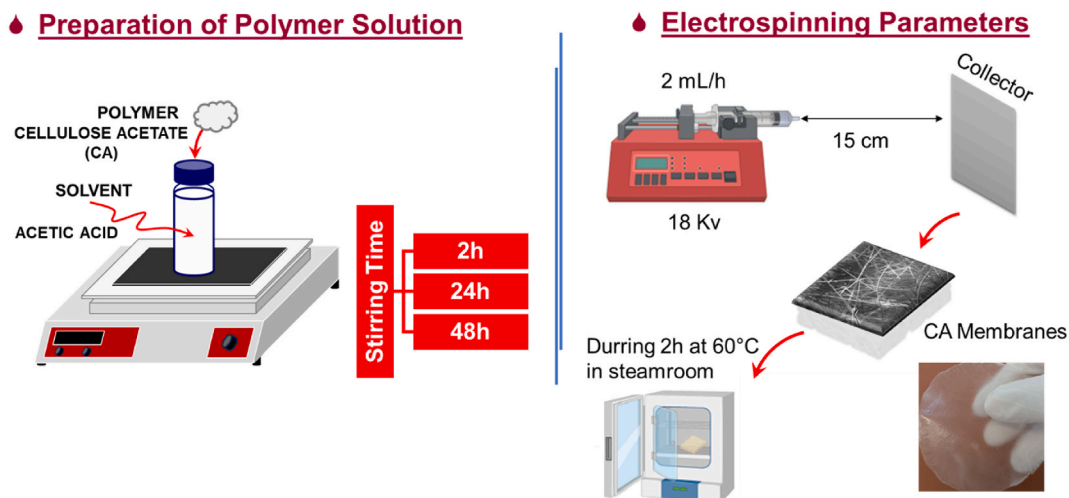


Fig. 1. Schematic diagram of synthetic of CA membrane synthesis.

where J_w is the ultrapure water flux ($L m^{-2} h^{-1}$) and Lp^0 the permeability of the solvent. It is determined by the solvent viscosity (η) and the membrane morphological properties (porosity, specific surface area, etc). The ΔP is the transmembrane pressure and R_m is the hydraulic membrane resistance (m^{-1}).

2.4.2. Resistance of CA nanofibers membranes to water

A surface of 2×2 cm² of CA membrane was weighted then it was immersed for 24 h in 50 mL of distilled water at room temperature. The membrane's weight was calculated after soaking for 24 h. The following equation was used to determine the membrane weight loss in percentage terms (W (%)) after being dispersed in water:

$$W (\%) = \frac{M_1 - M_2}{M_1} \times 100 \quad (3)$$

where M_1 represents the initial weight of the elaborated membrane and M_2 the membrane weight following a 24-h immersion in water.

2.4.3. Affinity based dye removal efficiency

Ultra violet (UV) visible absorption Spectrophotometer (Thermospectronic UV1, serial number: 501S13031802) was used to assess the quantitative study of affinity-based removal of IC dye in the wavelength range between 400 and 800 nm. The performance of elaborated membranes was tested at various concentrations (1, 2, 5 mg. L⁻¹) of IC dye.

The decolorization of dye solution was assessed by measuring the absorbance at the wavelength $\lambda_{max} = 610$ nm determined by UV-visible spectroscopy. The color removal was determined using the following equation [40]:

$$\text{Color removal (\%)} = \frac{ABS_0 - ABS_t}{ABS_0} \quad (4)$$

where ABS_0 is the absorbance of the initial dye solution and ABS_t denotes the absorbance of the dye after treatment with different CA membranes.

A schematic presentation of nanofiltration set-up and the performance evaluation process of the fabricated membranes are illustrated in Fig. 2.

3. Results and discussion

3.1. Morphology of cellulose membranes

The resulting morphology of the electrospun nanofibers is determined by the combined effects of solution property such as the molecular weight, concentration, conductivity, solvent volatility, and viscosity of the polymer as well as the processing parameters for instance: the needle tip placement and design, the applied voltage, the flow rate and the tip-to-collector separation. Therefore, altering these parameters will directly influence the size and fiber morphology [41]. Concerning viscosity and solution homogeneity, they are impacted by varying the stirring time during the electrospinning process. The ideal stirring duration depends on the polymer-solvent system and the required fiber properties. Both longer and shorter stirring times have different effects on the electrospinning process. In most cases, electrospinning requires experimentation and systematic optimization to determine the optimal conditions for reaching the desired fiber diameter [42]. The representative SEM images of synthesized CA membranes as a function of the stirring time of the electrospun solution are shown in Fig. 3. As it can be observed, for lower stirring time particularly 2 h, the synthesized CA nanofiber

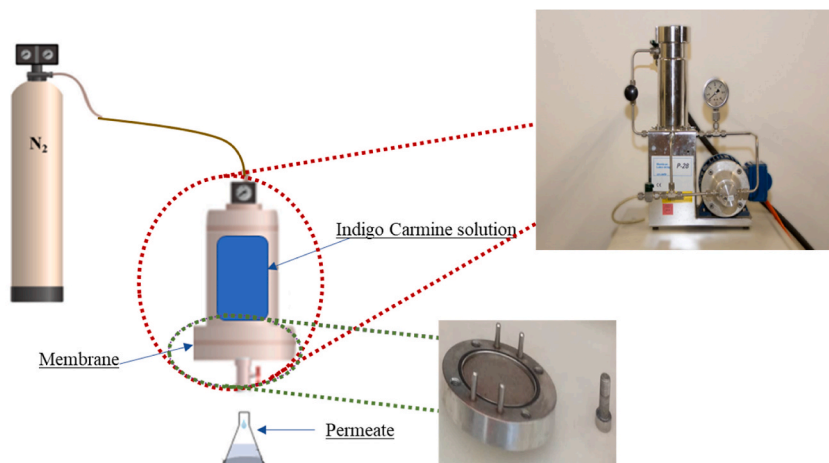
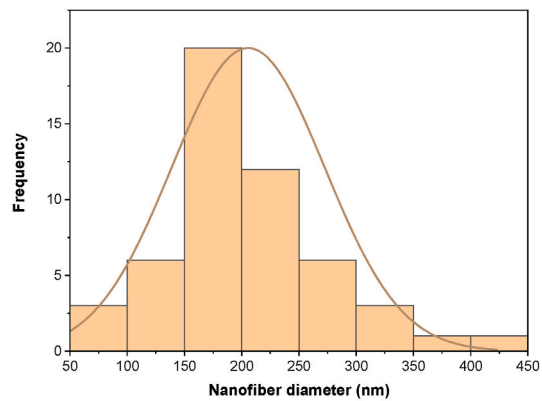
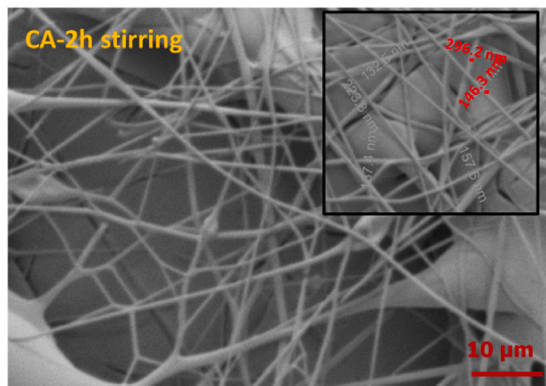
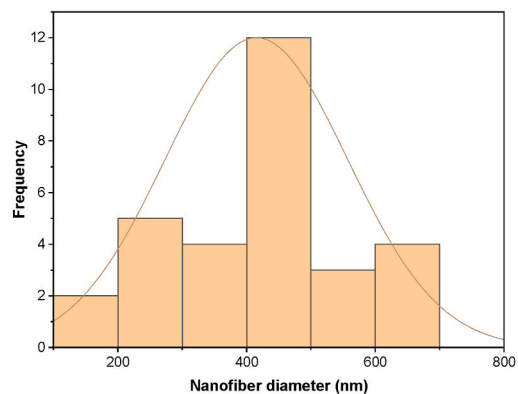
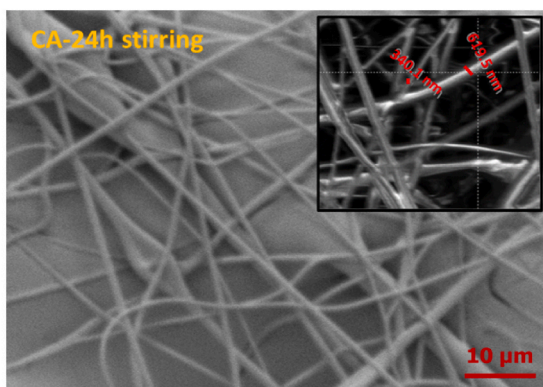


Fig. 2. A schematic of nano-filtration set-up.

(a)



(b)



(c)

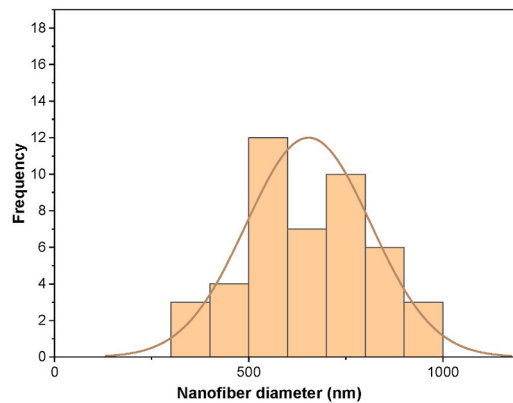
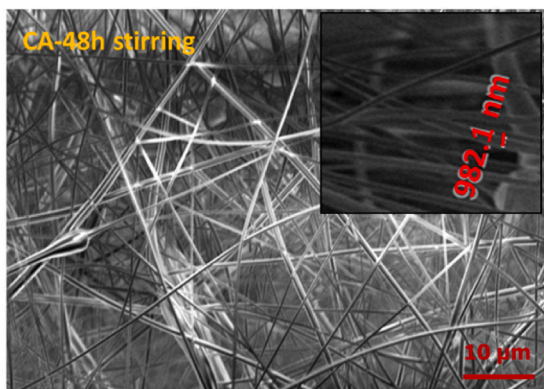


Fig. 3. SEM images and histogram diagrams of the CA nanofibers as function with stirring time (a) 2 h, (b) 24 h and (c) 48 h.

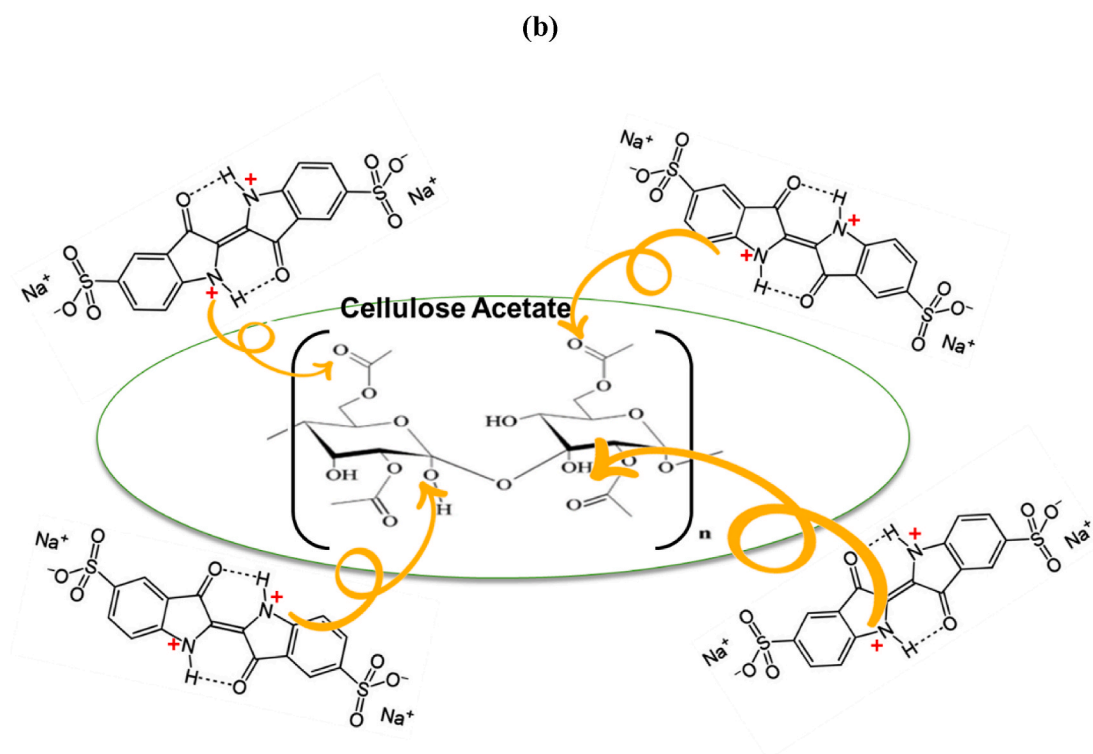
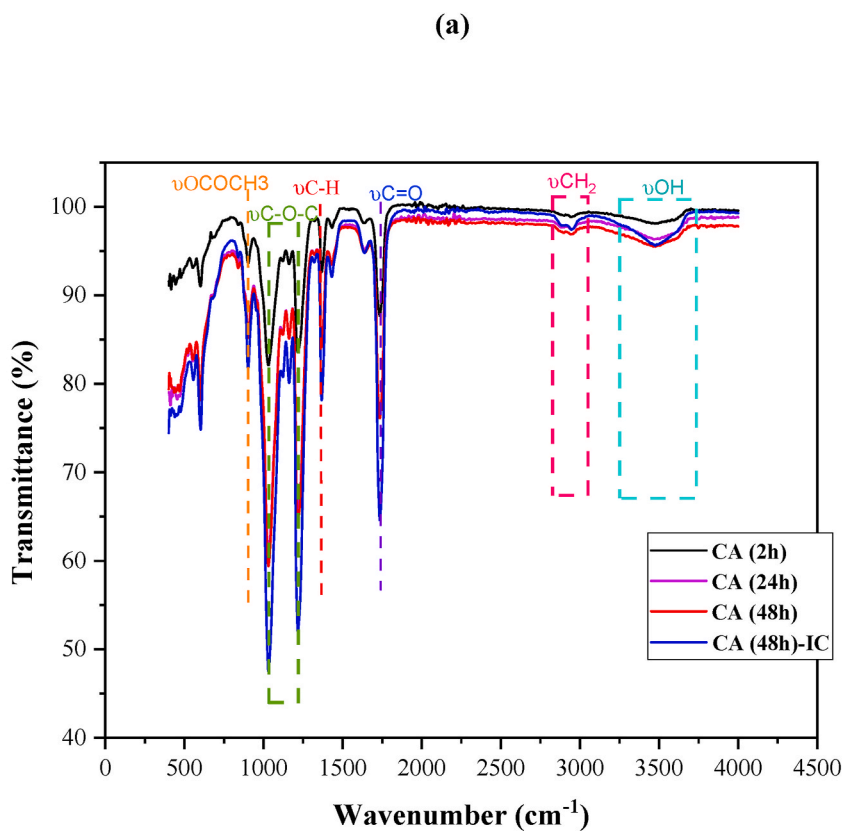


Fig. 4. FT-IR spectra of the CA membranes before and after adsorption of IC dye.

membranes have some irregular nanofibers with a diameter size ranging from $350 \text{ nm} \pm 50 \text{ nm}$ – $950 \text{ nm} \pm 50 \text{ nm}$. Indeed, insufficient mixing during short stirring periods could lead to an unequal dispersion of polymer chains within the mixture. This lack of homogeneity can lead to variations in fiber diameter. Longer periods of stirring cause an increase of solution viscosity, which augments the resistance to stretching and elongation during the electrospinning process. This behavior can lead to greater nanofiber diameters. As seen, the SEM images displayed an increase of CA nanofibers diameter to $950 \text{ nm} \pm 50 \text{ nm}$ with 48 h stirring (histograms of fiber diameter distribution in Fig. 3). Likewise, through the produced nanofibers, micro- and meso-pores in the nanofiber structure may be seen. From conducted experiments, we can denote that the homogeneity of CA solution can intensely affect the balance between the nucleation and the growth of nanofibers, resulting in a considerable modification of the final CA nanofibers shape. This behavior agrees with the previously reported results of Ghorani et al. [2015] [43]. Therefore, it is necessary to preserve the continuity of the jet throughout the electrospinning process for uniform nanofibers formation by mean of appropriate stirring duration.

3.2. FT-IR analysis

Fourier transform infrared spectroscopy was used to analyze the chemical structure of the obtained CA membranes. The FTIR spectrum (Fig. 4(a)) shows the typical absorption features of CA membranes in acetic acid. The strong characteristic absorption peaks at 1739 cm^{-1} ($\nu_{\text{C=O}}$, carbonyl stretch), 1377 cm^{-1} (methyl $\nu_{\text{C-H}}$ symmetric/asymmetric bend), 1219 cm^{-1} , 1028 cm^{-1} ($\nu_{\text{C-O-C}}$, alkoxy ester stretch) and 899 cm^{-1} ($\nu_{\text{O-C-O}}$) which are attributed to the vibrations of acetate group were observed [2,44]. Also, a broad absorption band at $3300\text{--}3500 \text{ cm}^{-1}$ corresponding to stretching of OH group and an absorption band at $2700\text{--}2900 \text{ cm}^{-1}$ related to $-\text{CH}_2$ groups were detected [45]. This analysis verifies the interfacial polymerization of CA and confirms nanofiber creation during the electrospinning process. For FTIR analysis after IC dye adsorption (Fig. 4(a)), the spectrum of CA (48 h)-IC shows the existence of characteristic bands of IC dye molecule in the region between ($900\text{--}1250 \text{ cm}^{-1}$) which can be assigned to the $-\text{SO}_3$ functional group present in dye structure [37]. The bands intensity of CA nanofiber membranes after IC dye adsorption increase especially for OH, C=O and C-N bands. The observed shift in peak values may be due to the bonding of the IC dye onto the CA adsorbent surface [46]. Based on the FTIR studies, a schematic representation of the possible adsorption mechanism has been shown in Fig. 4 (b).

3.3. Contact angle measurement

Contact angle measurement is considered as a simple experimental technique used for quantifying the chemical construction [47]. Editing the surface hydrophilicity-hydrophobicity is an important issue to consider when assessing the application field for electrospun CA membranes eventually in wastewater treatment. The swelling of CA nanofibers can influence the pore size and subsequently their response during wastewater treatment. To investigate the wettability of CA nanofibers, water contact angle measurements were studied, as shown in Fig. 5. It was analyzed that when stirring time increases, the capacity of water absorbency was reduced. Indeed, CA molecular chain contains hydrophilic hydroxyl groups but also hydrophobic groups which are not exposed to the surface of the electrospun nanofibers [48]. Here, the hydrophilicity of CA nanofibers was reduced because of the hydrophobic acetyl groups are being exposed to the nanofibers surface. When improving CA solution homogeneity by stirring, the percentage of hydrophobic side chains in the CA is augmented [49–51]. Consequently, the improvement of the CA solution homogeneity before electrospinning process is an important factor which contributes to the rise in contact angle values. This behavior gives more selectivity during filtration process [52]. It is important to note that the extent of the changes on CA molecular chain depends not only on the duration and conditions of the hydrolysis reaction but also on the concentration of acetic acid used. These parameters can be optimized to achieve the desired properties of the final material [53,54].

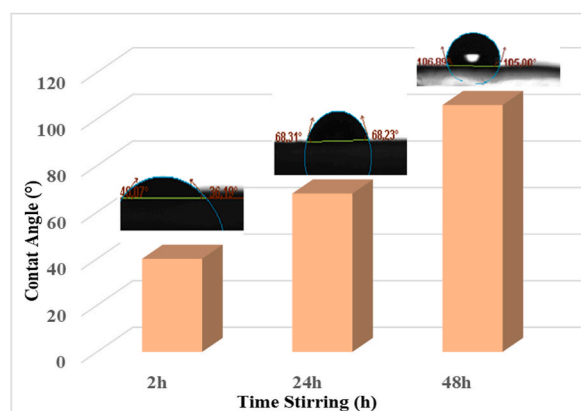


Fig. 5. Variation of the Contact Angle of CA electrospun membranes as a function of stirring time.

3.4. Water permeability flux

Fig. 6 shows the obtained water permeation fluxes (PWF) for different elaborated membranes. The presented curves exhibit a linear aspect with the slope of the permeability L^0_p as a function of pressure. As indicated in Fig. 6, the L^0_p is found to correspond to the range of the nanofiltration membrane. It is also noticeable from Fig. 6 that the PWF of different CA membranes increased respectively with the stirring time increase. According to experimental results, the PWF of CA (48 h), CA (24 h) and CA (2 h) is 97.30 L/h m² bar, 46.39 L/h m² bar and 28.79 L/h m² bar, respectively. The augmentation of stirring time engenders an increase in ultrapure water permeability, which might be explained by improved nanofibers structure after 48 h stirring. Indeed, the CA solution homogeneity influences the pore-formatting mechanism, which directly influences membrane porosity and results in a higher flux. Similar trends were previously reported in the literature [39,55,56].

3.5. Water resistance of CA nanofibers membranes

Water resistance of produced CA membranes is described in Fig. 7 (a). It shows that the resistance to water was greatly increased by CA solution stirring augment. This behavior might be related to the stability of achieved membrane (48 h) even after immersion in water for 24 h. This stability might be related to the enhanced nanofiber structure [39].

3.6. Nanofiltration applied to wastewater treatment

Due to their porosity, large specific surface area and ease of regeneration, electrospun membranes offer a viable material for adsorbing pollutants from aqueous solutions [57–59]. Moreover, the nanofibers layered structure gives the nanoparticles unique charges and functional groups with more adsorption sites, accelerating thereby the rate and capacity of adsorption. Due to their toxicity, slow rate of degradation, and stability on water bodies, concerns about dye molecules in wastewaters are very serious [60]. Thus, significant research efforts have been made to focus on the mechanism of dye removal with electrospun membranes [61].

Within this section, the influence of electrospun solution homogeneity on the membrane has been demonstrated. To explore the importance of this crucial parameter, the nanofiltration efficiency of the different green elaborated CA electrospun nanofibers membranes for various concentrations of IC dye are detailed in Fig. 8. The color removal efficiency for the concentration 1 mg/L was found approximately 28 %, 50 % and 65 % with CA (2 h), CA (24 h) and CA (48 h), respectively.

On the other hand, the color removal of 2 mg/L reached about 31 %, 40 % and 78 % for the same membranes, respectively. Besides, 42 %, 74 % and 83 % for the concentration 5 mg/L. Definitely, by increasing stirring time, the membrane morphology is enhanced (regular fiber diameter, no beads, pore size distribution) and consequently, the nanofiltration efficiency showed a similar improvement consequently. Meanwhile, the increase of the applied pressure from 0 bar to 12 bar raises also color removal efficiency. These later constatations agree with suggested explanations.

Based on the FTIR analysis, the mechanism of dye adsorption was attributed to functional groups in CA, which may act as sites for physical adsorption. Hydrogen bonds and electrostatic force of attraction may be additional factors. Furthermore, the achieved hydrophobic character of CA nanofibers prepared with 48 h time of stirring, especially the acetyl group, can reinforce the surface adsorption towards the active surface. Therefore, the number of available adsorption sites on the membrane surface is supported which conducts to the improvement of nanofiltration of IC dye [62,63]. As a matter of fact, the adsorption rate at higher concentrations of IC dye may be influenced by the diffusion of molecules that exchange ions within the CA membrane.

Table .1 displays a comparison of the maximum adsorption capacity (Q_m) of various membranes toward IC studied in other works. The maximum adsorption capacity reported (13.09 mg/g) for elaborated CA membranes is attained for CA nanofibers prepared with 48 h stirring. Comparing to other studies, it is clear that the elaborated CA nanofiber membranes have good adsorption capacity than that obtained with other adsorbents. Subsequently, the elaborated neat polymer CA nanofiber membrane is a promising nanomaterial for dye removal from industrial textile wastewater.

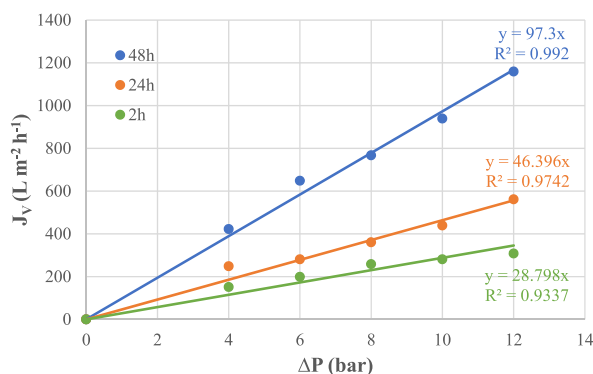


Fig. 6. Water permeate fluxes of CA membranes as a function with pressure.

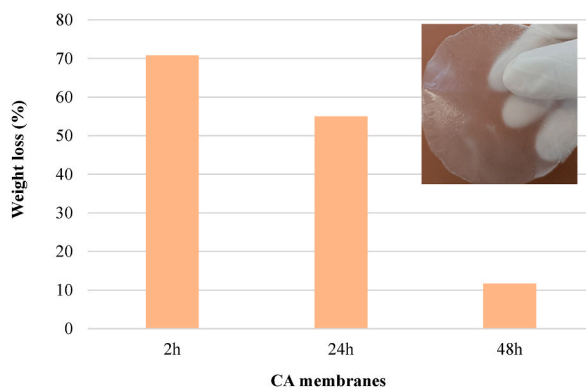


Fig. 7. Water resistance of the CA nanofibers membranes.

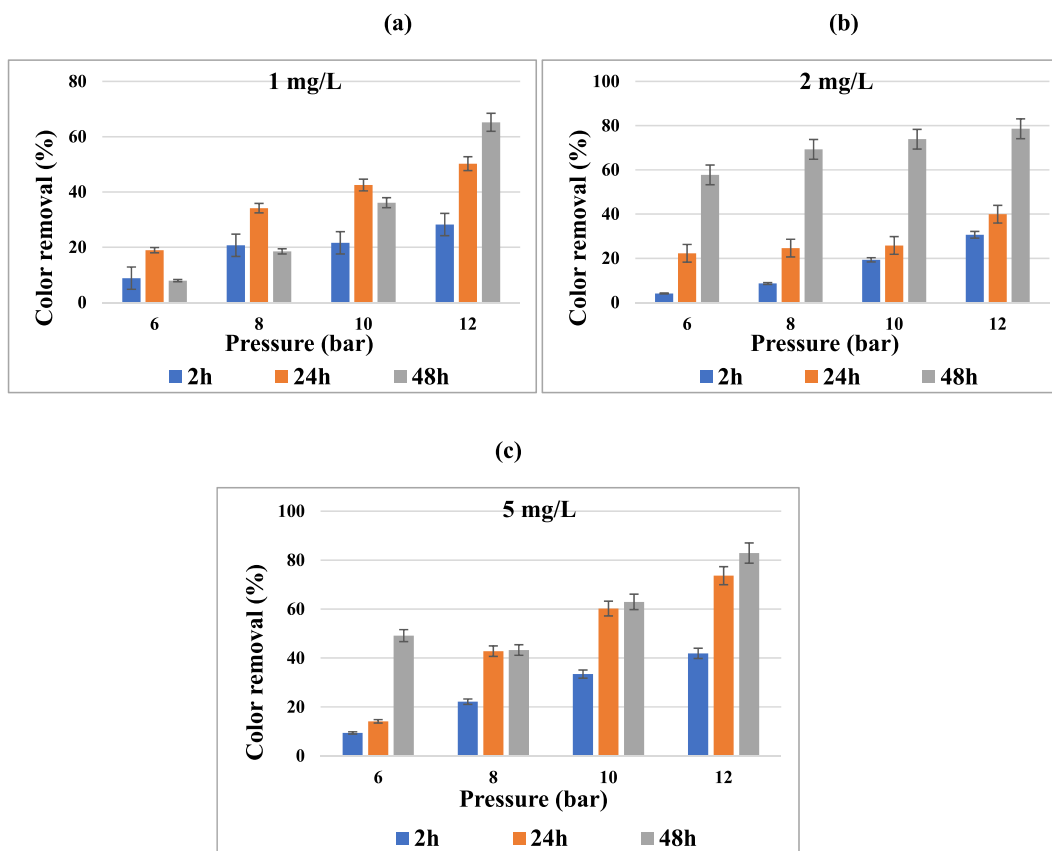


Fig. 8. Color removal of Indigo Carmine dye using different CA membrane samples as a function with concentrations (1 mg/L, 2 mg/L and 5 mg/L) and with applied pressure.

Table 1

Comparison of CA nanofibers prepared with 48 h stirring time adsorption capacity with other adsorbents for removal of IC dye.

Adsorbent	Maximum adsorption capacity Q_m (mg/g)	References
CA-48 h	13.09 mg/g	This work
Chitin	5.8 mg/g	[64]
Glutaraldehyde cross-linked chitosan	1.8 mg/g	[65]
Calcium hydroxide	0.95 mg/g	[66]
Polyvinylidene fluoride (PVDF)	12.5 mg/g	[67]

4. Conclusions and prospects

The ability of membranes made from electrospun CA nanofibers to eliminate IC dye was examined in this study. These nanofiber membranes enormous surface areas are suitable for removing certain compounds through physical adsorption. For membrane elaboration, we considered the acetic acid as solvent and crosslinking agent to lower the hydrophilic structure of CA nanofiber. In fact, this hydrophilic character can engender quite low adsorptions. To enhance membranes performance in dye sorption, we varied the stirring time (2 h, 24 h and 48 h) during solution preparation to study its effect on solution homogeneity. The obtained membranes exhibited a good uniformity and nanofibers were well defined with stirring time increase. Furthermore, the decrease of hydrophilic character is reached because of the esters groups hydrolysis within CA polymer while reaction with acetic acid. As reaction progress, as the proportion of acetate groups decreases, which leads to a proportional decrease in water absorption capacity and a change in the wetting properties of CA. Consequently, membranes with optimized parameters attained a percentage of 83 % color removal of 5 mg/L concentration at 12 bar as a maximum of adsorption capacity of IC ($Q_m = 13.09$ mg/g). Therefore, these green elaborated nanomaterials could open a new path for removing color molecules from textile effluents. The performance of membranes can also be enhanced by further research to develop modified nanofibrous adsorption materials that immobilize functional groups or fillers on the fiber network. It is also necessary to look at the stability and degradability of these electrospun nanofibers as well as the migration of nanofillers.

Additionally, by immobilizing the functional groups or fillers on the fiber network, these fibrous adsorption materials are intended to create a readily manipulable nanomaterial with a large number of binding sites. It would be vital to know that the electrospun adsorbents won't add any additional impurities to the water system or environment.

Data availability statement

The data used in the current study is available upon request from the corresponding author. However, the data associated with our study has not been deposited into a publicly available repository.

CRedit authorship contribution statement

Ines Elaiassaoui: Writing – original draft, Data curation. **Soumaya Sayeb:** Methodology, Investigation. **Ibtissem Ounif:** Resources. **Mounir Ferhi:** Formal analysis. **Dorra Jellouli Ennigrou:** Visualization, Validation, Supervision, Project administration, Conceptualization.

Declaration of competing interest

All authors don't have received any funding, grants, for the preparation of the manuscript.

All authors don't have association or financial involvement with any organization or commercial entity having a financial interest in or financial conflict with the subject matter or research presented in the manuscript.

Acknowledgements

Authors acknowledge Agency for the Promotion of Scientific Research (ANPR) (Tunisia) for providing financial support to accomplish this research work within the framework of the MOBIDOC device financed by the European Union within the framework of the PROMESSE program.

References

- [1] X. Xiao, Y. Sun, W. Sun, H. Shen, H. Zheng, Y. Xu, J. Zhao, H. Wu, C. Liu, Advanced treatment of actual textile dye wastewater by Fenton-flocculation process, *Can. J. Chem. Eng.* 95 (2016) 1245–1252, <https://doi.org/10.1002/cjce.22752>.
- [2] D. Lv, R. Wang, G. Tang, Z. Mou, J. Lei, J. Han, D.S. Smedt, R. Xiong, Ch Huang, Ecofriendly electrospun membranes loaded with visible-light-responding nanoparticles for multifunctional usages: highly efficient air filtration, dye scavenging, and bactericidal activity, *ACS Appl. Mater. Interfaces* 11 (2019) 12880–12889, <https://doi.org/10.1021/acsami.9b01508>.
- [3] D. Hu, H. Zhao, G. Feng, C. Wang, Y. Li, Fabrication of nanofiltration membranes through the deposition of polyethyleneimine on SMA-polyethersulfone supports under acid catalysis for cationic dye/salt separation, *J. Environ. Chem. Eng.* 11 (2023) 111055, <https://doi.org/10.1016/j.jece.2023.111055>.
- [4] Q.M. Khan, D. Kharaghani, S. Ullah, M. Waqas, R.M.A. Abbasi, Y. Saito, Ch Zhu, S.I. Kim, Cleaning properties of electrospun PVA/TiO₂ and PVA/ZnO nanofibers composites, *Nanomaterials* 8 (2018) 644, <https://doi.org/10.3390/nano8090644>.
- [5] S. Gopi, P. Balakrishnan, A. Pius, S. Thomas, Chitin nanowhisker (ChNW)- functionalized electrospun PVDF membrane for enhanced removal of Indigo carmine, *Carbohydr. Polym.* 165 (2017) 115–122.
- [6] N.R. Appiah, A.F. Baye, B.T. Gadisa, M.W. Abebe, H. Kim, In-situ prepared ZnO-ZnFe₂O₄ with 1-D nanofiber network structure: an effective adsorbent for toxic dye effluent treatment, *J. Hazard Mater.* 373 (2019) 459–467, <https://doi.org/10.1016/j.jhazmat.2019.03.108>.
- [7] L.A. Mercante, M.H.M. Facure, D.A. Locilento, R.C. Sanfelice, F.L. Migliorini, H.C. Mattoso, D.S. Correa, Solution blow spun PMMA nanofibers wrapped with reduced graphene oxide as an efficient dye adsorbent, *New J. Chem.* 41 (2017) 9087–9094, <https://doi.org/10.1039/C7NJ01703K>.
- [8] S. Rethinam, B.S. Kavukcu, T. Hemalatha, W.A. Aruni, A. Sendemir, C. Turkey, Cellulose based electrospun nanofilters: perspectives on tannery effluent wastewater treatment, *Cellulose* 29 (2022) 1969–1980, <https://doi.org/10.1007/s10570-022-04420>.
- [9] I. Elaiassaoui, H. Akrouf, S. Grassini, D. Fulginiti, L. Bousselmi, Effect of coating method on the structure and properties of a novel PbO₂ anode for electrochemical oxidation of Amaranth dye, *Chemosphere* 217 (2019) 26–34, <https://doi.org/10.1016/j.chemosphere.2018.10.161>.
- [10] T. Lou, X. Yan, X. Wang, Chitosan coated polyacrylonitrile nanofibrous mat for dye adsorption, *Int. J. Biol. Macromol.* 135 (2019) 919–925, <https://doi.org/10.1016/j.ijbiomac.2019.06.008>.

- [11] Z. Hua, L. Tang, M. Wu, J. Fu, Graphene hydrogel improves *S. putrefaciens*' biological treatment of dye wastewater: impacts of extracellular electron transfer and function of c-type cytochromes, *Environ. Res.* 236 (2023) 116739, <https://doi.org/10.1016/j.envres.2023.116739>.
- [12] L.R. Manea, A. Berdea, A. Popa, A.P. Berdea, Electrospun membranes for environmental protection IOP conf. Ser, *Mater. Sci. Eng.* 374 (2018) 012081, <https://doi.org/10.1088/1757-899X/374/1/012081>.
- [13] R. Guo, R. Wang, J. Yin, T. Jiao, H. Huang, X. Zhao, L. Zhang, Q. Li, J. Zhou, Q. Peng, Fabrication and highly efficient dye removal characterization of beta-cyclodextrin-based composite polymer fibers by electrospinning, *Nanomaterials* 9 (2019) 127, <https://doi.org/10.3390/nano9010127>.
- [14] F. Guo, Y. Miao, L. Xu, Q. Zhou, T. Deng, Conductive thin-film nanocomposite nanofiltration membrane comprising N-doped graphene quantum dots with relieved concentration polarization for sulfate separation from high-salinity solution, *Desalination* 555 (2023) 116526, <https://doi.org/10.1016/j.desal.2023.116526>.
- [15] W. Zhang, P. Yang, X. Li, Z. Zhu, M. Chen, X. Zhou, Electrospun lignin-based composite nanofiber membrane as high-performance absorbent for water purification, *Int. J. Biol. Macromol.* 141 (2019) 747–755, <https://doi.org/10.1016/j.ijbiomac.2019.08.221>.
- [16] M.N. Collins, M. Nechifor, F. Tanasă, M. Zănoagă, A. McLoughlin, M.A. Stróżyk, M. Culebras, C.A. Teacă, Valorization of lignin in polymer and composite systems for advanced engineering applications – a review, *Int. J. Biol. Macromol.* 131 (2019) 828–849, <https://doi.org/10.1016/j.ijbiomac.2019.03.069>.
- [17] R. Senthil, B. Basaran, S. Vijayan, A. Mert, O. Bayraktar, A.A. Wilson, Electrospun nano-bio membrane for bone tissue engineering application- a new approach, *Mater. Chem. Phys.* 249 (2020) 123010, <https://doi.org/10.1016/j.matchemphys.2020.123010>.
- [18] Y. Yin, Y. Guang, H. Zhang, Q. Xia, C. Wang, Synergistic effect of POSS and chitosan on highly enhancing the separation selectivity and antifouling capacity of polyamide membranes, *Desalination* 573 (2024) 117215, <https://doi.org/10.1016/j.desal.2023.117215>.
- [19] F. Ahmed, A.A. Arbab, A.W. Jatoi, M. Khatri, N. Memon, Z. Khatri, I.S. Kim, Ultrasonic-assisted deacetylation of cellulose acetate nanofibers: a rapid method to produce cellulose nanofibers, *Ultrason. Sonochem.* 36 (2017) 319–325, <https://doi.org/10.1016/j.matchemphys.2020.123010>.
- [20] Y. Zhang, F. Wang, Y. Wang, Electrospun cellulose acetate/chitosan fibers for humic acid removal: construction guided by intermolecular interaction study, *ACS Appl. Polym. Mater.* 3 (2021) b 5022–5029, <https://doi.org/10.3390/nano12081284>.
- [21] C. Wang, J. Yin, R. Wang, T. Jiao, H. Huang, J. Zhou, L. Zhang, Q. Peng, Facile preparation of self-assembled polydopamine-modified electrospun fibers for highly effective removal of organic dyes, *Nanomaterials* 9 (2019) 116, <https://doi.org/10.3390/nano9010116>.
- [22] J. Ding, X. Ding, C. Wu, Y. Wu, S. Xia, Phospho-modified polyamide nanofiltration membranes with high permeability by using alendronate sodium as additives, *Desalination* 573 (2024) 117188, <https://doi.org/10.1016/j.desal.2023.117188>.
- [23] A.A. Hamad, M.S. Hassouna, T.I. Shalaby, M.F. Elkady, A.M.A. Elkawi, H.A. Hamad, Electrospun cellulose acetate nanofiber incorporated with hydroxyapatite for removal of heavy metals, *Int. J. Biol. Macromol.* 151 (2020) 1299–1313, <https://doi.org/10.1016/j.ijbiomac.2019.10.176>.
- [24] L. Francis, R.A. Al-Juboori, M. Khatri, N. Hilal, Nanostructured nanofiltration hollow fiber membranes for metal recovery from industrial wastewater, *J. Water Process Eng.* 56 (2023) 104281, <https://doi.org/10.1016/j.jwpe.2023.104281>.
- [25] X. Zhan, R. Ge, T. Huo, J. Lu, J. Li, Highly permeable PA@GO loose nanofiltration membranes enabled by hierarchical transport channels for efficient dye removal, *Chem. Eng. J.* 476 (5) (2023) 146831, <https://doi.org/10.1016/j.cej.2023.146831>.
- [26] Y. Liu, C. Hou, T. Jiao, J. Song, X. Zhang, R. Xing, J. Zhou, L. Zhang, Q. Peng, Self-assembled AgNP-containing nanocomposites constructed by electrospinning as efficient dye photocatalyst materials for wastewater treatment, *Nanomaterials* 8 (2018) 35, <https://doi.org/10.3390/nano8010035>.
- [27] Y. Zhang, Y. Wang, Electrospun cellulose-acetate/chitosan fibers for humic-acid removal: improved efficiency and robustness with a core-sheath design, *Nanomaterials* 12 (2022) 1284, <https://doi.org/10.3390/nano12081284>.
- [28] Y. Zhang, F. Wang, Y. Wang, Recent developments of electrospun nanofibrous materials as novel adsorbents for water treatment, *Mater. Today Commun.* 27 (2021) 102272, <https://doi.org/10.1016/j.mtcomm.2021.102272>.
- [29] K. Khan, S. Masroor, G. Rizvi, Electrospinning and electrospun based polyvinyl alcohol nanofibers utilized as filters and sensors in the real world, *J. Polym. Eng.* 43 (2023) 627–663, <https://doi.org/10.1515/polyeng-2023-004>.
- [30] J. Lee, S. Moon, J. Lahann, K.J. Lee, Recent progress in preparing nonwoven nanofibers via needleless electrospinning, *Macromol. Mater. Eng.* 308 (2023) 2300057, <https://doi.org/10.1002/mame.202300057>.
- [31] V. Raja, L. Mahalakshmi, M.M. Leena, J.A. Moses, C. Anandharamkrishnan, Needleless electrospinning: concepts and applications in the food industry, *Food Eng. Rev.* (2023), <https://doi.org/10.1007/s12393-023-09362-2>.
- [32] R. Bilginer, A.A. Yildiz, A facile method to fabricate propolis enriched biomimetic PVA architectures by co-electrospinning, *Mater. Lett.* 276 (2020) 128191, <https://doi.org/10.1016/j.matlet.2020.128191>.
- [33] G. El-Barbary, M.K. Ahmed, M.M. El-Desoky, M.A. Al-Enizi, A.A. Alothman, M.A. Alotaibi, A. Nafady, Cellulose acetate nanofibers embedded with Ag nanoparticles/CdSe/graphene oxide composite for degradation of methylene blue, *Synth. Met.* 278 (2021) 116824, <https://doi.org/10.1016/j.synthmet.2021.116824>.
- [34] A. Rhimi, K. Zlaoui, N.K. Horchani, E.D. Jellouli, Characterization and extraction of sodium alginate from Tunisian algae: synthesizing a cross-linked ultrafiltration membrane Iran, *Polym. J.* 31 (2022) 367–382, <https://doi.org/10.1007/s13726-021-01005-09>.
- [35] A. Mansourizadeh, A.J. Azad, Preparation of blend polyethersulfone/cellulose acetate/polyethylene glycol asymmetric membranes for oil-water separation, *J. Polym. Res.* 21 (2014) 375, <https://doi.org/10.1007/s10965-014-0375-x>.
- [36] M.G. Yazdi, M. Ivanic, Alaa Mohamed, A. Uheida, Surface modified composite nanofibers for the removal of indigo carmine dye from polluted water, *RSC Adv.* 8 (2018) 24588, <https://doi.org/10.1039/c8ra02463d>.
- [37] J. Zolgharnein, F. Rajabali, S.D. Farahani, Indigo carmine dye adsorptive removal by polyethylene glycol-modified hydroxyapatite nanoparticles as an efficient adsorbent, *Water Air Soil Pollut.* (2023) 234, <https://doi.org/10.1007/s11270-023-06207-w>, 210.
- [38] L. Jiang, K. Li, H. Yang, X. Liu, W. Li, W. Xu, B. Deng, Improving mechanical properties of electrospun cellulose acetate nanofiber membranes by cellulose nanocrystals with and without polyvinylpyrrolidone, *Cellulose* 27 (2020) 955–967, <https://doi.org/10.1007/s10570-019-02830-1>.
- [39] S. Tahazadeh, T. Mohammadi, A.M. Tofighy, S. Khanlari, H. Karimi, M.B.H. Emrooz, Development of cellulose acetate/metal-organic framework derived porous carbon adsorptive membrane for dye removal applications, *J. Membr. Sci.* 638 (2021) 119692, <https://doi.org/10.1016/j.memsci.2021.119692>.
- [40] I. Elaissoui, H. Akrouf, S. Grassini, D. Fulginiti, L. Bousselemi, Role of SiO_x interlayer in the electrochemical degradation of Amaranth dye using SS/PbO₂ anodes, *Mater. Des.* 110 (2016) 633–643, <https://doi.org/10.1016/j.matdes.2016.08.044>.
- [41] W. Ma, Z. Guo, J. Zhao, Q. Yu, F. Wang, J. Han, H. Pan, J. Yao, Q. Zhang, S.K. Samal, S.C. De Smedt, C. Huang, Polyamide/cellulose acetate core/shell electrospun fibrous membranes for oil-water separation, *Sep. Purif. Technol.* 177 (2017) 71–85, <https://doi.org/10.1016/j.seppur.2016.12.032>.
- [42] A.M. Anjeh, S.R. Nabavi, Preparation, characterization and properties of a novel electrospun polyamide-6/chitosan/graphene oxide composite nanofiber, *J. Polym. Environ.* 30 (2022) 3934–3948, <https://doi.org/10.1007/s10924-022-02485-3>.
- [43] B. Ghorani, P. Goswami, S.J. Russell, Parametric study of electrospun cellulose acetate in relation to fibre diameter, *RJTA* 19 (2015) 24–40, <https://doi.org/10.1108/RJTA-19-04-2015-B003>.
- [44] I. Ounifi, Y. Guesmi, C. Ursino, R. Castro-Muñoz, H. Agougui, M. Jabli, A. Hafane, A. Figoli, E. Ferjani, Synthesis and characterization of a thin-film composite nanofiltration membrane based on polyamide-cellulose acetate: application for water, *Purification. J. Polym. Environ.* (2021), <https://doi.org/10.1007/s10924-021-02233-z>.
- [45] T.A. Saleh, M. Tuzen, A. Sari, Polyamide magnetic palygorskite for the simultaneous removal of Hg (II) and methyl mercury; with factorial design analysis, *J. Environ. Manag.* 211 (2018) 323–333, <https://doi.org/10.1016/j.jenvman.2018.01.050>.
- [46] F. Ebrahimi, S.R. Nabavi, A. Omrani, Fabrication of hydrophilic hierarchical PAN/SiO₂ nanofibers by electrospay assisted electrospinning for efficient removal of cationic dyes, *Environ. Technol. Innovat.* 25 (2022) 102258, <https://doi.org/10.1016/j.eti.2021.102258>.
- [47] K.H. Mah, H.W. Yusoff, M.A. Seman, A.W. Mohammad, Polyester thin film composite nanofiltration membranes via interfacial polymerization: influence of five synthesis parameters on water permeability, *J. Mech. Eng. Sci.* 12 (2018) 3387–3398, <https://doi.org/10.15282/jmes.12.1.2018.8.0302>.
- [48] M. Mubashir, Y.Y. Fong, C.T. Leng, L.K. Keong, Enhanced gases separation of cellulose acetate membrane using N-methyl-1-2 pyrrolidone as fabrication solvent, *Int. J. Automot. Mech. Eng.* 15 (2018) 4978–4986, <https://doi.org/10.15282/IJAME.15.1.2018.7.0386>.

- [49] C.Y.Y. Tang, Y.N. Kwon, J.O. Leckie, Effect of membrane chemistry and coating layer on physiochemical properties of thin film composite polyamide RO and NF membranes II. Membrane physiochemical properties and their dependence on polyamide and coating layers, *Desalination* 242 (2009) 168–182, <https://doi.org/10.1016/j.desal.2008.04.003>.
- [50] M. Faraji, S.R. Nabavi, H.S. Kenari, Fabrication of a PAN–PA6/PANI membrane using dual spinneret electrospinning followed by *in situ* polymerization for separation of oil-in-water emulsions, *New J. Chem.* 44 (2020) 13488–13500, <https://doi.org/10.1039/D0NJ03231J>.
- [51] Y. Aitomäki, S. Moreno-Rodriguez, T.S. Lundström, K. Oksman, Vacuum infusion of cellulose nanofibre network composites: influence of porosity on permeability and impregnation, *Mater. Des.* 95 (2016) 204–211, <https://doi.org/10.1016/j.matdes.2016.01.060>.
- [52] Q. Zhang, T.M. Young, D.P. Harper, T. Liles, S. Wang, Optimization of electrospun poly(vinyl alcohol)/cellulose nanocrystals composite nanofibrous filter fabrication using response surface methodology, *Carbohydr. Technol. Appl.* 2 (2021) 100120, <https://doi.org/10.1016/j.carpta.2021.100120>.
- [53] L.A. Goetz, N. Naseri, S.S. Nair, Z. Karim, A.P. Mathew, All cellulose electrospun water purification membranes nanotextured using cellulose nanocrystals, *Cellulose* 25 (2018) 3011–3023, <https://doi.org/10.1007/s10570-018-1751-1>.
- [54] X. Zhao, C. Huanga, S. Zhanga, C. Wang, Cellulose acetate/activated carbon composite membrane with effective dye adsorption performance, *J. Macromol. Sci. B.* 58 (2019) 909–920, <https://doi.org/10.1080/00222348.2019.1669945>.
- [55] N. Jalalian, S.R. Nabavi, Electrospayed chitosan nanoparticles decorated on Polyamide6 electrospun nanofibers as membrane for acid fuchsin dye filtration from water, *Surface. Interfac.* 21 (2020) 100779, <https://doi.org/10.1016/j.surf.2020.100779>.
- [56] N. Maximous, G. Nakhla, W. Wan, Comparative assessment of hydrophobic and hydrophilic membrane fouling in wastewater applications, *J. Membr. Sci.* 339 (2009) 93–99, <https://doi.org/10.1016/j.memsci.2009.04.034>.
- [57] Y. Chen, Y. Qiu, W. Chen, Q. Wei, Electrospun thymol-loaded porous cellulose acetate fibers with potential biomedical applications, *Mater. Sci. Eng. C* 109 (2020) 110536, <https://doi.org/10.1016/j.msec.2019.110536>.
- [58] R.T. Thomas, J.I.D.R. Vicente, K. Zhang, M. Karzarjehdi, H. Liimatainen, K. Oksman, Size exclusion and affinity-based removal of nanoparticles with electrospun cellulose acetate membranes infused with functionalized cellulose nanocrystals, *Mater. Des.* (2022) 217110654, <https://doi.org/10.1016/j.matdes.2022.110654>.
- [59] F. Zou, G. Li, X. Wang, A.L. Yarin, Dynamic hydrophobicity of superhydrophobic PTFE–SiO₂ electrospun fibrous membranes, *J. Membr. Sci.* (2021), <https://doi.org/10.1016/j.memsci.2020.118810>.
- [60] H. Ma, C. Burger, B.S. Hsiao, B. Chu, Nanofibrous microfiltration membrane based on cellulose nanowhiskers, *Biomacromolecules* 13 (2012) 180–186, <https://doi.org/10.1021/bm201421g>.
- [61] C.I.I. Bates, E. Loranger, A.P. Mathew, B. Chabot, Cellulose reinforced electrospun chitosan nanofibers bio-based composite sorbent for water treatment applications, *Cellulose* 28 (2021) 4865–4885, <https://doi.org/10.1007/s10570-021-03828-4>.
- [62] P.R. Sharma, S.K. Sharma, T. Lindström, B.S. Hsiao, Nanocellulose-enabled membranes for water purification: perspectives, *Adv. Sustain. Syst.* (2020) 1900114, <https://doi.org/10.1002/advs.201900114>.
- [63] D.N. Phan, M.Q. Khan, N.T. Nguyen, T.T. Phan, A. Ullah, M. Khatri, N.N. Kien, I.S. Kim, A review on the fabrication of several carbohydrate polymers into nanofibrous structures using electrospinning for removal of metal ions and dyes, *Carbohydr. Polym.* 252 (2021) 117175, <https://doi.org/10.1016/j.carbpol.2020.117175>.
- [64] A.G.S. Prado, J.D. Torres, E.A. Faria, S.C.L. Dias, Comparative adsorption studies of indigo carmine dye on chitin and chitosan, *J. Colloid Interface Sci.* 277 (2004) 43–47, <https://doi.org/10.1016/j.jcis.2004.04.056>.
- [65] A.R. Cestari, E.F.S. Vieira, A.M.G. Tavares, R.E. Bruns, The removal of the indigo carmine dye from aqueous solutions using cross-linked chitosan— evaluation of adsorption thermodynamics using a full factorial design, *J. Hazard Mater.* 153 (2008) 566–574, <https://doi.org/10.1016/j.jhazmat.2007.08.092>.
- [66] T.N. Ramesh, D.V. Kirana, A. Ashwini, T.R. Manasa, Calcium hydroxide as low-cost adsorbent for the effective removal of indigo carmine dye in water, *J. Saudi Chem. Soc.* 21 (2017) 165–171, <https://doi.org/10.1016/j.jscs.2015.03.001>.
- [67] S. Gopia, P. Balakrishnan, A. Pius, S. Thomas, Chitin nanowhisker (ChNW)-functionalized electrospun PVDF membrane for enhanced removal of Indigo carmine, *Carbohydr. Polym.* 165 (2017) 115–122, <https://doi.org/10.1016/j.carbpol.2017.02.046>.